THE JOURNAL OF BIOLOGICAL CHEMISTRY VOL. 287, NO. 18, pp. 14502–14514, April 27, 2012
© 2012 by The American Society for Biochemistry and Molecular Biology, Inc. Published in the U.S.A.

The Role of CD38 in Fcγ Receptor (FcγR)-mediated Phagocytosis in Murine Macrophages*

Received for publication, November 29, 2011, and in revised form, February 23, 2012 Published, JBC Papers in Press, March 6, 2012, DOI 10.1074/jbc.M111.329003

John Kang[‡1], **Kwang-Hyun Park**[‡§1,2], **Jwa-Jin Kim**[¶], **Eun-Kyeong Jo**[¶], **Myung-Kwan Han**[§‖], **and Uh-Hyun Kim**[‡§3]

From the [‡]*Department of Biochemistry,* [‖]*Department of Microbiology,* [§]*Institute for Medical Sciences, Chonbuk National University Medical School, Jeonju, 561-180, Korea and the* [¶]*Department of Microbiology, Chungnam National University School of Medicine, Daejeon 301-747, Korea*

Background: Ca^{2+} signaling in FcγR-mediated phagocytosis is unclear.
Results: We show that FcγR-mediated phagocytosis requires the production of cyclic ADP-ribose by CD38.
Conclusion: CD38 plays a crucial role for Ca^{2+} signaling in FcγR-mediated phagocytosis.
Significance: This study provides new perspectives in immune defense and can help shed light on developing novel methods or drugs for manipulating bacterial infections.

Phagocytosis is a crucial event in the immune system that allows cells to engulf and eliminate pathogens. This is mediated through the action of immunoglobulin (IgG)-opsonized microbes acting on Fcγ receptors (FcγR) on macrophages, which results in sustained levels of intracellular Ca^{2+} through the mobilization of Ca^{2+} second messengers. It is known that the ADP-ribosyl cyclase is responsible for the rise in Ca^{2+} levels after FcγR activation. However, it is unclear whether and how CD38 is involved in FcγR-mediated phagocytosis. Here we show that CD38 is recruited to the forming phagosomes during phagocytosis of IgG-opsonized particles and produces cyclic-ADP-ribose, which acts on ER Ca^{2+} stores, thus allowing an increase in FcγR activation-mediated phagocytosis. Ca^{2+} data show that pretreatment of J774A.1 macrophages with 8-bromo-cADPR, ryanodine, blebbistatin, and various store-operated Ca^{2+} inhibitors prevented the long-lasting Ca^{2+} signal, which significantly reduced the number of ingested opsonized particles. *Ex vivo* data with macrophages extracted from $CD38^{-/-}$ mice also shows a reduced Ca^{2+} signaling and phagocytic index. Furthermore, a significantly reduced phagocytic index of *Mycobacterium bovis* BCG was shown in macrophages from $CD38^{-/-}$ mice *in vivo*. This study suggests a crucial role of CD38 in FcγR-mediated phagocytosis through its recruitment to the phagosome and mobilization of cADPR-induced intracellular Ca^{2+} and store-operated extracellular Ca^{2+} influx.

The catalysis of the substrate NAD^+ to Ca^{2+} second messenger, cyclic ADP-ribose (cADPR),[4] is made possible through the action of the type II transmembrane glycoprotein CD38 due to its ADP-ribosyl (ADPR) cyclase activity (1, 2). Once production is initiated, cyclic ADP-ribose (cADPR) can then act on ryanodine receptors (RyR) located on endoplasmic reticulum/sarcoplasmic reticulum (ER/SR) stores, which will ultimately lead to an increase in intracellular Ca^{2+} levels ($[Ca^{2+}]_i$) via Ca^{2+} release in many different types of cells (3–5). This rise in $[Ca^{2+}]_i$ is responsible for various mechanisms in immune cells, and it has been implicated in chemotaxis (6), cell adhesion (7), and cytokine secretion (8).

CD38 can also generate another Ca^{2+} signaling messenger nicotinic acid adenine dinucleotide phosphate (NAADP) depending on the cell system (9, 10). Like cADPR, NAADP can be very potent in eliciting a rise in $[Ca^{2+}]_i$ by acting on receptors of specific Ca^{2+} stores that are insensitive to thapsigargin (11–13). It has been suggested that these stores are lysosome-related acidic organelles that can provide a long-lasting $[Ca^{2+}]_i$ increase similar to ER stores (14–16).

One of the intriguing aspects of CD38 is what is known as the "topological paradox," where the active site of CD38 is located outside of the cellular membrane (17). This begs to ask the question of how CD38 can catalyze the production of its messengers cADPR and NAADP because the substrates NAD/NADP as well as the targets for cADPR/NAADP are present intracellularly. It has been suggested that connexin 43 hemichannels, a component of the gap junction, mediate cADPR generation in the extracellular space or intracellular vesicles and its approach to ryanodine receptor by NAD/cADPR transport (18). It has also been suggested that CD38 is internalized once activated via endocytosis, thus allowing its catalytic site to interact with intracellular substrates (19–21). This internalizing event has been observed in many different cellular responses where cADPR production is shifted from the surface to inside the cell (22, 23). It has been suggested that the internalization mechanism is mediated by non-muscle myosin heavy chain IIA (MHCIIA), where both CD38 and MHCIIA

* This work was supported by Korea Science and Engineering Foundation (National Research Laboratory Grant R0A-2007-000-20121-0) (to U.-H. K.).
[1] Both authors contributed equally to this work.
[2] Present address: Department of Oriental Pharmaceutical Development, Nambu University, Gwangju, 506–706, Korea.
[3] To whom correspondence should be addressed: Dept. of Biochemistry, Chonbuk National University Medical School, Keumam-dong, Jeonju, 561-182, Republic of Korea. Tel.: 82-63-270-3083; Fax: 82-63-274-9833; E-mail: uhkim@chonbuk.ac.kr.
[4] The abbreviations used are: cADPR, cyclic ADP-ribose; ER, endoplasmic reticulum; SR, sarcoplasmic reticulum; NAADP, nicotinic acid ADP; MHCIIA, myosin heavy chain IIA; RyR, ryanodine receptor; FcγR, Fcγ receptor; IP_3, inositol trisphosphate; HBSS, Hanks' balanced salt solution; NGD, nicotinamide guanine dinucleotide; *M. bovis* BCG, *M. bovis* Bacille de Calmette Guerin; cGDPR, cyclic GDP-ribose; SOCE, store-operated Ca^{2+} entry; LB, latex beads; TRITC, tetramethylrhodamine isothiocyanate.

were found to be associated in activated lymphokine-activated killer cells (24). Phagocytosis is the mechanism of internalization used by phagocytes to internalize and degrade microorganisms, cell debris, and various particles (25). We have previously reported the possible role of CD38 in Fcγ receptors (FcγR)-stimulated phagocytosis where extracellular NAD can help regulate this event in the J774A.1 cell line (26). Thus, there is a possibility that CD38 internalization is related to FcγR-mediated phagocytosis, but there currently have been no studies on CD38 internalization in FcγR-mediated phagocytosis.

Early studies have shown that the accumulation of $[Ca^{2+}]_i$ may even be responsible for conducting phagocytosis by controlling many different phenomenon such as phagosomal maturation (26–28), cytoskeletal rearrangements (29–31), and phagosome-lysosome fusion (32). There are many different types of receptors on the surface of macrophages that can initiate phagocytosis, such as complement receptors (33, 34), mannose receptors (35, 36), Sp-A receptors (37), scavenger receptors (38), and subfamilies of FcγR. It has been hypothesized that the binding of immunoglobulin-opsonized pathogens with FcγR on the plasma membrane is a major factor in mediating this Ca^{2+} response (39). This was first seen when Ca^{2+} signals were detected during phagocytosis of opsonized targets in a variety of immune cells (40–43).

Within the FcγR family, there are four different classes of FcγRs, FcγRI, FcγRII, FcγRIII, and FcγRIV, where macrophages are known to express all four classes (44, 45). Once initiated, the FcγRs will cluster on the outer membrane of macrophages and commence the phosphorylation of immunoreceptor tyrosine-based activation motifs by Src family tyrosine kinases. The phosphorylated immunoreceptor tyrosine-based activation motifs will then gather a variety of signaling enzymes and complexes, which will start a signaling cascade that ultimately leads to phagocytosis (46, 47). At this point Syk and PI3K kinases can be activated. Syk in particular can then phosphorylate phospholipase Cγ, which then cleaves membrane phospholipid phosphatidylinositol 4,5-diphosphate into inositol trisphosphate (IP_3) and diacylglycerol (46–48), where the former binds to Ca^{2+} channels on the ER that allows Ca^{2+} release into the cytosol (49). Any additional Ca^{2+} signaling that is possibly involved afterward at this point in macrophage phagocytosis has not yet been explored.

In this study we show that CD38 is recruited and internalized to the phagosome containing IgG-opsonized particles and induces cADPR production, thereby resulting in intracellular Ca^{2+} increase and FcγR-stimulated phagocytosis enhancement. In addition, we show that CD38 knock-out reduces FcγR-stimulated phagocytosis in murine macrophages and inhibits phagocytosis of *Mycobacterium bovis* BCG in mice. Our results suggest that CD38 is involved in the host's defense to bacterial infection.

EXPERIMENTAL PROCEDURES

Materials and Reagents—Mouse IgG, 3.0-μm polystyrene latex beads, bovine serum albumin, Triton X-100, thioglycollate medium, 8-Br-cADPR, and streptavidine-Cy3 conjugate were purchased from Sigma. RPMI 1640 medium, DMEM medium, fetal bovine serum, trypsin, and antibiotics were purchased from HyClone Laboratories, Inc. (Logan, UT). Fluo-3 AM was purchased from Invitrogen. FITC-conjugated rat anti-mouse CD38 was purchased from BD Biosciences Pharmingen. Target retrieval solution and antibody diluent were purchased from Dako (Denmark). Xestospongin C, ryanodine, and blebbistatin were purchased from Calbiochem. Bafilomycin A1 and rabbit polyclonal MYH9 antibody were purchased from Santa Cruz Biotechnology (Santa Cruz, CA). Biotinylation of anti-*M. bovis* BCG polyclonal antibody was carried out through the technical service by Advanced Biochemicals Inc. (Jeonju, South Korea).

Animals—C57BL/6 mice were purchased from OrientBio (Sungnam, South Korea). CD38 knock-out mice were purchased from The Jackson Laboratory. Mice were bred and kept in animal housing facilities at Chonbuk National University Medical School under specific pathogen free (SPF) conditions. All experimental animals were used under a protocol approved by the institutional animal care and use committee of the Chonbuk National University Medical School. Standard guidelines for laboratory animal care were followed.

Cell Culture—The murine macrophage cell line J774A.1 (obtained from ATCC) and macrophages prepped from wild-type C57BL/6 and $CD38^{-/-}$ mice were maintained at 37 °C, 5% CO_2 in RPMI supplemented with 10% heat-inactivated FBS, 100 units/ml penicillin, and 100 μg/ml streptomycin. The cells were passaged weekly, and cells older than 15 passages were not used.

IgG-opsonized Latex Bead Preparation—Polystyrene latex beads (3.0 μm) were washed repeatedly with Hanks' balanced salt solution (HBSS) (1.5 mM $CaCl_2$, 145 mM NaCl, 5 mM KCl, 1 mM $MgCl_2$, 5 mM D-glucose, 20 mM HEPES, pH 7.3) and spun down at 1,700 rpm at 4 °C for 10 min. After washing, mouse IgG was added at a concentration of 3 mg/ml. The beads were then incubated at 4 °C on a rotator for 8 h to prevent any bead settling and to allow proper binding. After incubation, the beads were resuspended and washed repeatedly with cold buffer to remove any unbound IgG and kept on ice for immediate use.

TRITC IgG-opsonized Latex Bead Preparation—Soluble IgG was dialyzed with PBS at 4 °C for 2 h. The buffer was then replaced with 100 mM sodium carbonate buffer (10 mM Na_2CO_3, 90 mM $NaHCO_3$, pH 8.8), and the IgG solution was again dialyzed at 4 °C for an additional 2 h. TRITC was then added to the IgG solution and mixed thoroughly overnight at room temperature. For further purification and to separate any unbound TRITC, the IgG+TRITC solution was passed through a Sephadex G-75 column and collected. The amount of recovered TRITC-bound IgG was measured with a spectrophotometer at a wavelength of 280 nm. The appropriate amount of TRITC-bound IgG was opsonized to latex beads as mentioned in the above protocol. Polystyrene latex beads were washed repeatedly with HBSS and spun down at 1,700 rpm at 4 °C for 10 min. After washing, TRITC-bound IgG was added at a concentration of 3 mg/ml. The beads were then incubated at 4 °C on a rotator for 8 h. After incubation, the beads were resuspended and washed repeatedly with cold buffer to remove any unbound TRITC-bound IgG and kept on ice for immediate use.

Preparation of Polyclonal Antibody against M. bovis BCG—Rabbits were given an initial 1-ml subcutaneous injection of a crude sonically treated incomplete Freund's adjuvant (Sigma) mixture. Injections were given at five separate sites. Similarly prepared injections of 1 ml were repeated once after 1 month. Blood was obtained after 1 month, and the sera was isolated and designated as anti-BCG.

Immunohistochemistry—J774A.1 cells were plated on 24-well plates with coverslips at a density of 2.5×10^5 cells. Phagocytosis was initiated with TRITC-bound IgG-opsonized latex beads for 30 min at 37 °C in 5% CO_2 incubator. Cells were then immediately washed repeatedly with HBSS to remove any unbound beads and fixed with 3.7% paraformaldehyde solution for 1 h at 4 °C. The cells were then washed with PBS to remove excess paraformaldehyde and permeabilized with target retrieval solution according to the manufacturer's protocol. Cells were then washed with PBS and blocked with a filtered blocking buffer (1% BSA, 0.1% Triton X-100, 0.02% NaN_3 in PBS) at 4 °C for 1 h. Primary FITC-conjugated rat anti-mouse CD38 antibody or rabbit polyclonal MYH9 antibody were diluted with an antibody diluent (1:200) and incubated in the wells overnight at 4 °C. Wells were then washed repeatedly with TTBS (0.1 M Tris-HCl, pH 7.4, 150 mM NaCl, 0.1% Tween 20) with gentle shaking. Fluorochrome labeling to unconjugated antibodies were carried out through the technical service provided by Advanced Biochemicals Inc. (Jeonju, Korea). The stained cells were then exhaustively washed, and the coverslips were then removed and mounted on slides. The slides were viewed under a Carl-Zeiss confocal microscope (LSM 510 META, Jena, GmBH) at the Center for University-wide Research Facilities (Jeonju, Korea). For three-dimensional imaging, confocal Z-stacks (0.98 μm thick) were sequentially captured. Z-sections were combined into a *Z*-stack, and *XZ* sections/*YZ* sections of the *Z*-stack were reconstructed using the Zeiss LSM Image Browser (Version 4.2.0.121) to visualize internalized-molecule positioning in the cell.

Preparation of Mouse Macrophage—Briefly, each mouse was injected intraperitoneally with 2 ml of 3% thioglycollate medium. After 5 days the mice were sacrificed, and the thioglycollate-induced macrophages were extracted via peritoneal lavage with DMEM. The macrophages were centrifuged at 1500 rpm at 4 °C for 3 min and then resuspended at a cell concentration of 2×10^6 cells/ml with RPMI. Macrophages were plated in a 100-mm culture dish and kept in a 5% CO_2 incubator at 37 °C for 2 h. Non-adherent cells were then washed off with Dulbecco's phosphate-buffered saline (2.67 mM KCl, 1.47 mM KH_2PO_4, 137.93 mM NaCl, 8.06 mM $Na_2HPO_4 \cdot 7H_2O$), and the attached macrophages were kept in RPMI in a 5% CO_2 incubator at 37 °C. Isolated macrophages were used within 24 h.

Determination of ADPR Cyclase Activity—ADPR cyclase activity was determined fluorometrically using nicotinamide guanine dinucleotide (NGD^+) as a substrate (50). Phagocytosis was initiated in 2×10^6 cells per microtube at various time points with IgG-opsonized latex beads. The microtube-containing cells were incubated with 200 μM NGD^+, pH 7.2, at 4 °C for 30 min. The reaction was then stopped with 10% TCA, and the cells were pelleted by centrifugation. Fluorescence of cGDPR produced was determined at excitation/emission wavelengths of 297/410 nm (Hitachi F-2000).

Phagocytic Assay—J774A.1 cells were plated at a density of 1×10^6 cells/well in a 6-well plate overnight. The cells were pretreated with various nucleotides for 30 min at 37 °C in 5% CO_2 incubator. For phagocytosis, the media was removed and replaced with RPMI containing non-opsonized or IgG-opsonized latex beads for 30 min at 37 °C in 5% CO_2 incubator. The cells were then washed twice and fixed with 3.7% paraformaldehyde solution. Phagocytosis was assessed by light microscopy. Images were acquired by using a Nikon Eclipse TS100. Images acquired were captured using AVT-ActiveCam Viewer V1.1.0. The phagocytic index was calculated as follows: phagocytic index = number of latex beads internalized by 100 J774A.1 cells counted in 10 random fields.

Fluorometric Determination of Intracellular Ca^{2+} Concentration—J774A.1 cells or macrophages extracted from wild-type and $CD38^{-/-}$ C57BL/6 mice were washed twice with HBSS. Cells were then incubated with 5 μM Fluo-3 AM in HBSS at 37 °C for 30 min. The cells were washed three times with HBSS. Changes in fluorescence in the cells were determined at 488-nm excitation/530-nm emission by an air-cooled argon laser system. The emitted fluorescence at 530 nm was collected using a photomultiplier. One image was scanned every 4 s for 10 min using a confocal microscope (Nikon, Japan). For the calculation of $[Ca^{2+}]_i$, the method of Tsien *et al.* (51) was used with the equation, $[Ca^{2+}]_i = K_d(F - F_{min})/(F_{max} - F)$, where K_d is 488 nM for Fluo-3, and F is the observed fluorescence level. Each tracing was calibrated for the maximal intensity (F_{max}) by the addition of ionomycin (8 μM) and for the minimal intensity (F_{min}) by the addition of EGTA (50 mM) at the end of each measurement.

Isolation of Phagosome and Analysis—Cells were incubated with IgG-opsonized latex bead for 1 h with a multiplicity of infection at 50:1 and washed with PBS. After cell disruption using 30-gauge needle syringes, the latex bead containing phagosomes were isolated on a sucrose gradient (52, 53). The isolated phagosome was washed and resuspended with serum-free media for further use in experiments. For the identification of CD38 localization on the phagosome surface, latex bead-containing phagosomes were permeabilized with 0.1% Triton X-100 in serum-free media at 4 °C for 20 min and fixed with 4% paraformaldehyde. Thereafter, CD38 and MHCIIA were stained with specific antibodies. For immunoblotting, phagosome pellets were dissolved in 4% SDS in 50 mM Tris-HCl buffer, pH 8.0, by sonication. Solubilized proteins were obtained from the supernatant after centrifugation at 13,300 rpm for 20 min at 4 °C and were used for immunoblotting.

Measurement of Intracellular cADPR Concentration ($[cADPR]_i$)—cADPR was measured by some modification of the cycling method described previously (54). Briefly, after IgG-opsonized latex bead treatment to 2×10^6 cells/microtube at various time intervals, cells were treated with 0.6 M perchloric acid under sonication. Precipitates were removed by centrifugation at 14,000 rpm for 10 min at 4 °C. Perchloric acid was removed by mixing the aqueous sample with 3 parts 2 M $KHCO_3$ with vortex until the top aqueous layer containing cADPR cleared. The samples were then centrifuged at 14,000 rpm for 10 min at 4 °C. The top-most aqueous layer was col-

lected and neutralized with 0.1 M sodium phosphate, pH 8.0, mixed slightly by hand, and then let on ice. To remove all contaminating nucleotides including NAD but not cADPR, the samples were incubated with the following hydrolytic enzymes overnight at 37 °C: 0.44 units/ml nucleotide pyrophosphatase, 12.5 units/ml alkaline phosphatase, 0.0625 units/ml NADase, and 2.5 mM $MgCl_2$. Enzymes were removed by filtration using a centrifugal filter unit from Millipore (Billerica, MA) at 14,000 × *g* for 90 min. The filtrate was then collected for measurement of cADPR. To convert cADPR to β-NAD^+, the samples were incubated at room temperature for 1 h with the cycling reagent at a 2:1 ratio containing 0.3 μg/ml ADPR cyclase, 30 mM nicotinamide, and 20 mM sodium phosphate, pH 8.0. The samples were further incubated with a cycling reagent at 1:1 ratio containing 2% ethanol, 100 μg/ml alcohol dehydrogenase, 20 μM resazurin, 10 μg/ml diaphorase, 10 mM nicotinamide, 0.1 mg/ml BSA, 100 mM sodium phosphate pH 8.0, and 10 μM FMN. An increase in the resorufin fluorescence was measured at an excitation of 544 nm and an emission of 590 nm using a SpectraMax Gemini fluorescence plate reader (Molecular Devices Corp.) every 30 min for 3–4 h. Various known concentrations of cADPR were also included in the cycling reaction to generate a standard curve.

Measurement of Intracellular NAADP Concentration ($[NAADP]_i$)—The level of NAADP was measured using a cyclic enzymatic assay as described previously (55). Briefly, after IgG-opsonized latex bead treatment at various time intervals, cells were treated with 0.6 M perchloric acid under sonication. Precipitates were removed by centrifugation at 14,000 rpm for 10 min at 4 °C. Perchloric acid was removed by mixing the aqueous sample with 3 parts 2 M $KHCO_3$ with vortex until the top aqueous layer containing cADPR cleared. The samples were then centrifuged at 14,000 rpm for 10 min at 4 °C. The top-most aqueous layer was collected and neutralized with 0.1 M sodium phosphate, pH 8.0, mixed slightly by hand, and then let on ice. To remove all contaminating nucleotides, the samples were incubated with the following hydrolytic enzymes overnight at 37 °C: 2.5 units/ml apyrase, 0.125 units/ml NADase, 2 mM $MgCl_2$, 1 mM NaF, 0.1 mM PPi, and 0.16 mg/ml NMN-AT. Enzymes were removed by filtration using a centrifugal filter unit at 14,000 × *g* for 90 min. The filtrate was then collected for measurement of NAADP. For conversion of NAADP to NAAD, samples were incubated with 10 units/ml alkaline phosphatase overnight at 37 °C. Enzymes were then removed again by filtration. For conversion of NAAD to NAD, the samples were incubated at room temperature for 1 h with a cycling reagent at a 1:1 ratio containing 0.2 mg/ml NMN-AT, 0.2 mM NMN, 0.5 mM PPi, 10 nM nicotinamide, 2.0 mM NaF, 2.0 mM $MgCl_2$, and 100 mM Tris/HCl, pH 8.0. The samples were further incubated with a cycling reagent at 1:1 ratio containing 2% ethanol, 100 μg/ml alcohol dehydrogenase, 20 μM resazurin, 10 μg/ml diaphorase, 10 μM FMN, 0.1 mg/ml BSA, and 100 mM sodium phosphate, pH 8.0. An increase in the resorufin fluorescence was measured at an excitation of 544 nm and an emission of 590 nm using a SpectraMax Gemini fluorescence plate reader every 30 min for 3–4 h and once more overnight. Various known concentrations of NAADP were also included in the cycling reaction to generate a standard curve.

Statistical Analysis—Data represent the means ± S.E. of at least three separate experiments. Statistical analysis was performed using Student's *t* test. A value of $p < 0.05$ was considered significant.

RESULTS

IgG-opsonized Latex Beads Induce FcγR-mediated Phagocytosis via ADPR Cyclase Activation in J774A.1 Murine Macrophages—We first wanted to prove the possible presence and role of the transmembrane protein CD38 in J774A.1 macrophages during phagocytosis. We ascertained its expression using a NGD^+ assay that measures the formation of the fluorescent compound, cyclic GDP-ribose (cGDPR), as a result of its ADPR cyclase activity on the surface of the cells (Fig. 1*A*). We examined whether the enzyme activity was reduced by the internalization of CD38 through FcγR-mediated phagocytosis when adding IgG-opsonized 3.0-μm latex beads. This particular size of latex bead was chosen because it was found to have high levels of phagocytic cup formation and no lag in delivery to lysosomes (56). Almost immediately, after the addition of the opsonized beads, we found that the rate of formation of cGDPR significantly decreased over time with a greatest loss in activity at 15 s (Fig. 1*A*), but we did not observe reducing effect of cGDPR formation activity by non-opsonized latex beads, possibly due to the FcγR-mediated internalization of the ADPR cyclase from the plasma membrane for its activation. To visually show that particles can be internalized by FcγR-mediated phagocytosis, we treated J774A.1 macrophages with latex beads with or without opsonization of IgG by incubation for 30 min at 37 °C, and we saw that the IgG-opsonized beads had a dramatically higher rate of particle ingestion than the unopsonized beads (Fig. 1*B*). The phagocytosized ratio of non-opsonized LB was very low in comparison in J774.

For further confirmation we carried out an immunohistochemistry study where we stained for CD38 and MHCIIA (Fig. 2). To also verify that the ingested particles were indeed IgG-opsonized latex beads, we coated IgG with TRITC before opsonization. Not only did this make it easier to detect the phagocytosed bead, but it also confirmed that IgG was properly opsonized to the target. In the cell normal state, both CD38 and MHCIIA were found to be located mostly along the plasma membrane (Fig. 2, *A* and *B*). Once FcγR-mediated phagocytosis was initiated with IgG-opsonized latex beads, we found that both CD38 and MHCIIA seemed to internalize along with the opsonized bead (Fig. 2, *A* and *B*), confirming previous observations that CD38 is activated through internalization. We also observed the internalization of CD38 independently of the phagosome as well while also confirming that the IgG-opsonized latex beads themselves do not emit autofluorescence that could interfere with the immunohistochemistry interpretation (Fig. 2*C*). To determine the direction of the C terminus of CD38, which is the active site, we performed immunostaining with a C-terminal-specific antibody against CD38 (M-19, Santa Cruz) and anti-MHCIIA by permeabilization methods with a mild concentration of detergent. As a result, CD38 was not stained in non-permeabilized phagosomes and co-localized with the IgG-coated surface of the latex beads, whereas MHCIIA was stained in both groups with a similar pattern and co-localized with the

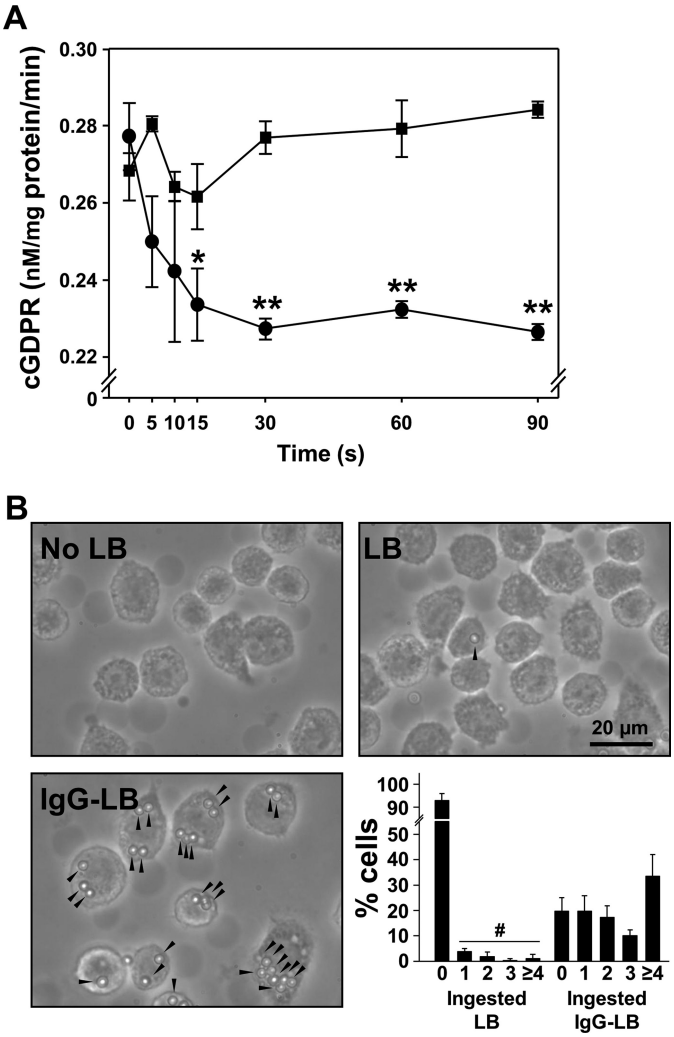

FIGURE 1. **IgG-opsonized latex beads induce FcγR-mediated phagocytosis via ADPR-cyclase activation in J774A.1 murine macrophages.** ADPR-cyclase activity was assessed in J774A.1 murine macrophages through an NGD^+ assay where 200 μM NGD^+ was used as a substrate as described in "Experimental Procedures." *A*, a decrease in ADPR-cyclase activity at the membrane surface was observed in a time-dependent manner after initiating FcγR-mediated phagocytosis with IgG-opsonized latex beads. The data represent the mean ± S.D. cGDPR formation of three experiments. $p < 0.05$ (*) *versus* zero time. $p < 0.01$ (**) *versus* zero time. *Closed squares* and *closed circles* are latex bead and IgG-opsonized latex bead groups, respectively. *B*, unaffected J774A.1 macrophages (*upper left panel*) were preincubated with 3.0 μm latex beads without IgG opsonization (*LB*) (*upper right panel*) or with IgG opsonization (*IgG-LB*) (*lower left panel*) for 30 min at 37 °C in 5% CO_2 (magnification ×40). *Lower right panel*, statistic analysis of phagocytosis in J774A.1 cells. $p < 0.001$ (#) *versus* no-ingested latex bead group of J774.A1 cells.

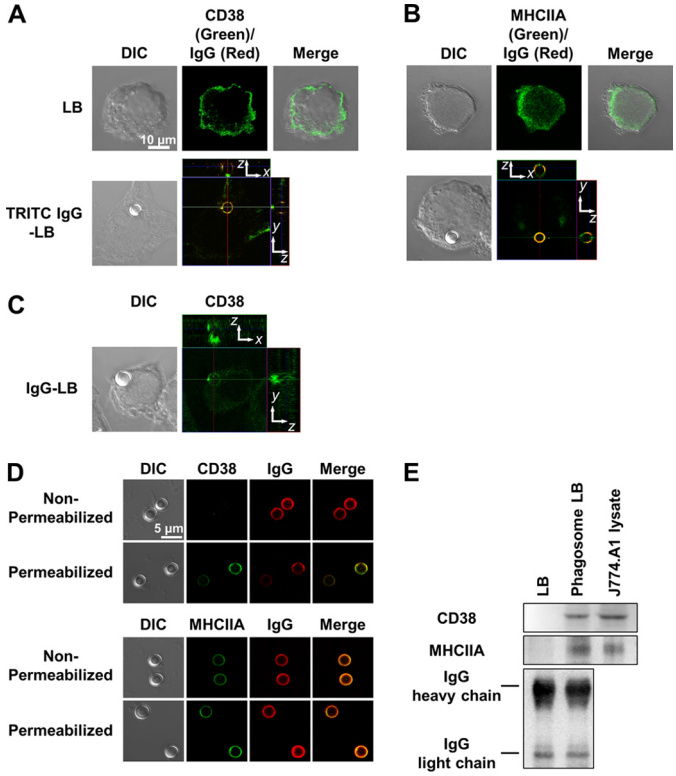

FIGURE 2. **Two or three-dimensional fluorescence images of CD38 and myosin heavy chain IIA in J774A.1 murine macrophages.** CD38 and MHCIIA internalization via FcγR-mediated phagocytosis was visualized through immunohistochemistry with a primary FITC-conjugated rat anti-mouse CD38 or a rabbit polyclonal MYH9 antibody, respectively, as described under "Experimental Procedures." *A*, CD38 (*green*) was found to be situated along the plasma membrane in its resting state (control). Initiation of FcγR-mediated phagocytosis with TRITC IgG-opsonized latex beads (*LB*, *red*) resulted in CD38 internalization where it co-localized with the phagosome. *DIC*, differential interference contrast. *B*, MHCIIA (*green*) was also found to be situated along the plasma membrane in its resting state (control). Initiation of FcγR-mediated phagocytosis with TRITC IgG-opsonized latex beads (*red*) resulted in MHCIIA internalization, where it also colocalized with the phagosome. *C*, CD38 (*green*) also internalizes independently of the phagosome after initiating FcγR-mediated phagocytosis with IgG-opsonized latex beads. The *blue line* shows the position of the phagosome on the *z* axis. The *x* (*green line*), *y* (*red line*) image is the confocal *z* axis slice corresponding to the position of the *blue line* (*i.e.* through the center of the phagosome). The phagosome is stably positioned within the cell. *D*, shown are co-localized images of CD38 or MHCIIA with phagocytosed-latex bead. Latex bead-containing phagosomes were isolated as described under "Experimental Procedures" and stained with anti-CD38 and anti-MHCIIA antibodies with or without permeabilization. *E*, shown is a Western blot of CD38 and IgG with biotinylated anti-CD38 antibody and anti-mouse IgG antibody on latex beads (*LB*), latex bead-containing phagosome (*phagosome LB*), and whole lysate of J774.A1 cells.

IgG-coated surface of the latex beads. CD38 on the phagosomes was distinguished by immunoblotting with a biotinylated anti-CD38 antibody and streptavidin-HRP. These results indicate that IgG-opsonized latex beads can elicit FcγR-mediated phagocytosis, which seems to be mediated by the ADPR cyclase CD38 via association with MHCIIA, and the C terminus of CD38 is localized in the lumen of phagosomes.

IgG-coated Latex Beads Induce Ca^{2+} Signaling in J774A.1 Macrophages—After witnessing the possible involvement of an ADPR cyclase, we delved deeper into its action by performing Ca^{2+} signaling experiments and measuring the changes in intracellular Ca^{2+}. The Ca^{2+}-sensitive fluorescent dye Fluo-3 AM was used with or without pretreatment of a variety of classical Ca^{2+} signaling inhibitors in J774A.1 macrophages before introducing IgG-opsonized latex beads. The addition of IgG-opsonized latex beads alone without any inhibitors was able to generate typical long-lasting Ca^{2+} signals (Fig. 3*A*). To see if IP_3 is utilized in the Ca^{2+} signaling pathway of FcγR-mediated phagocytosis, we pretreated the cells with 2 μM xestospongin C, an IP_3 receptor blocker (57), and found that this had no affect on the Ca^{2+} signal (Fig. 3*B*), suggesting that IP_3 is not involved. We previously reported that extracellular cADPR enhanced FcγR-mediated phagocytosis (25). To corroborate our previous finding that cADPR is involved in FcγR-mediated phagocytosis, we pretreated our cells with a 100 μM concentration of an antagonistic analog of cADPR, 8-Br-cADPR (58), and we observed that preincubation with this inhibitor was able to

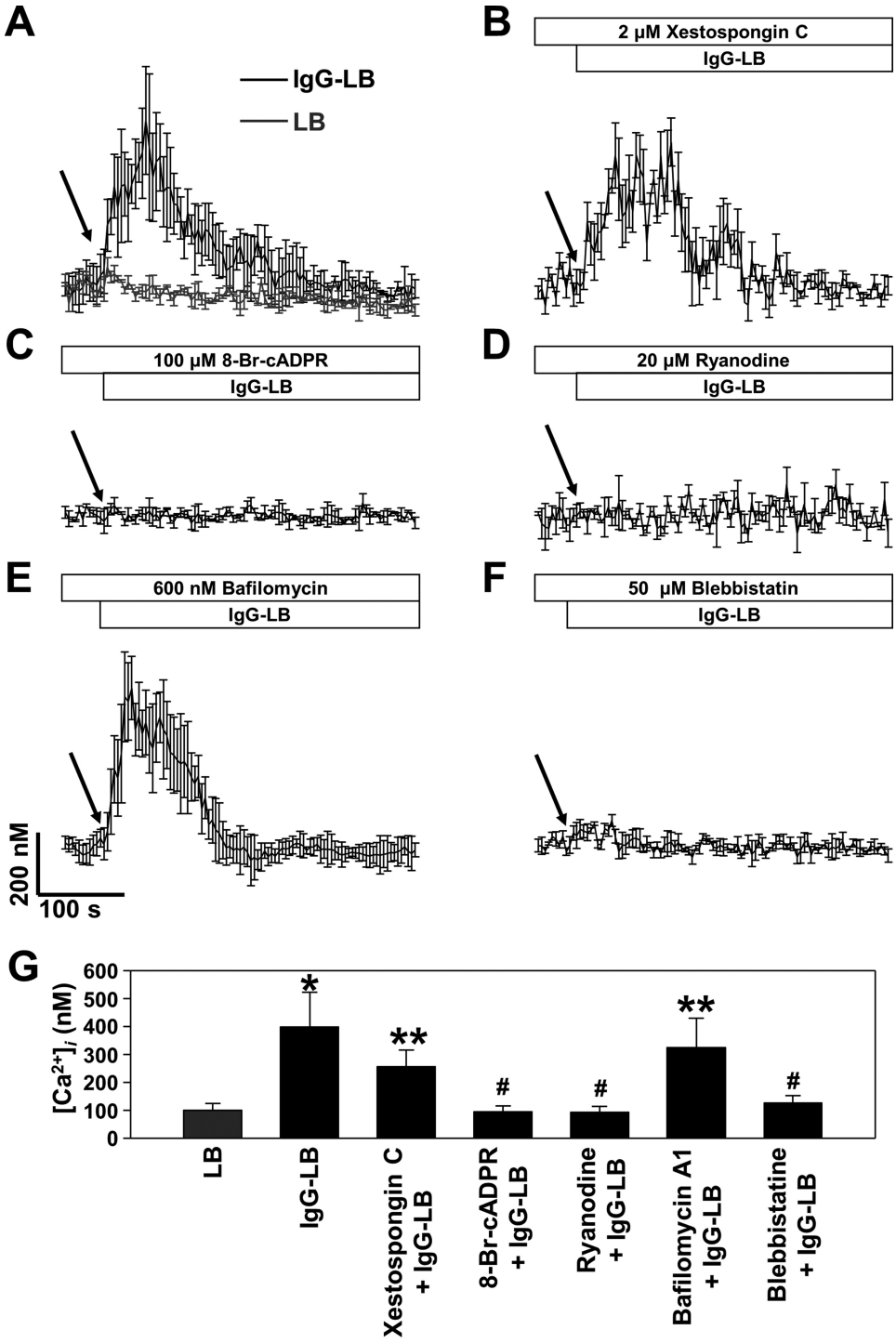

FIGURE 3. **IgG-opsonized latex beads induce Ca^{2+} signaling in J774A.1 murine macrophages.** $[Ca^{2+}]_i$ measurements in FcγR stimulation was determined by a confocal microscope on J774A.1 cells preincubated with Fluo-3 AM as described under "Experimental Procedures." *A*, IgG-opsonized latex beads induces a rapid rise in $[Ca^{2+}]_i$, whereas unopsonized latex beads do not elicit Ca^{2+} signaling. Shown is the effect of 2 μM xestospongin C (*B*), 100 μM 8-Br-cADPR (*C*), 20 μM ryanodine (*D*), 600 nM bafilomycin A1 (*E*), and 50 μM blebbistatin (*F*) on FcγR stimulation-induced $[Ca^{2+}]_i$ increase in J774A.1 murine macrophages. *Arrows* indicate time point of un/opsonized latex bead addition. *G*, a direct comparison of Ca^{2+} levels at 15 s after treatment of latex beads (*LB*) or IgG-LB. Each line represents the mean ± S.D. of $[Ca^{2+}]_i$ from minimum three independent experiments. $p < 0.01$ (*) and $p < 0.05$ (**) *versus* LB treated group; $p < 0.01$ (#) *versus* IgG-LB group.

abolish the long-lasting Ca^{2+} signal (Fig. 3*C*). cADPR is also known to act on ryanodine receptor for Ca^{2+} release (59). For additional confirmation we used 20 μM ryanodine, as it antagonistically binds to ryanodine receptor on ER/SR Ca^{2+} stores (60). We discovered that this provided very similar results as with 8-Br-cADPR, thus providing some consistency (Fig. 3*D*). Because NAADP is known to be synthesized by CD38, we wanted to see its potential role by preincubating our cells with 600 nM bafilomycin A1, a vacuolar H^+-ATPase inhibitor that is required for maintaining acidity of NAADP-sensitive Ca^{2+}

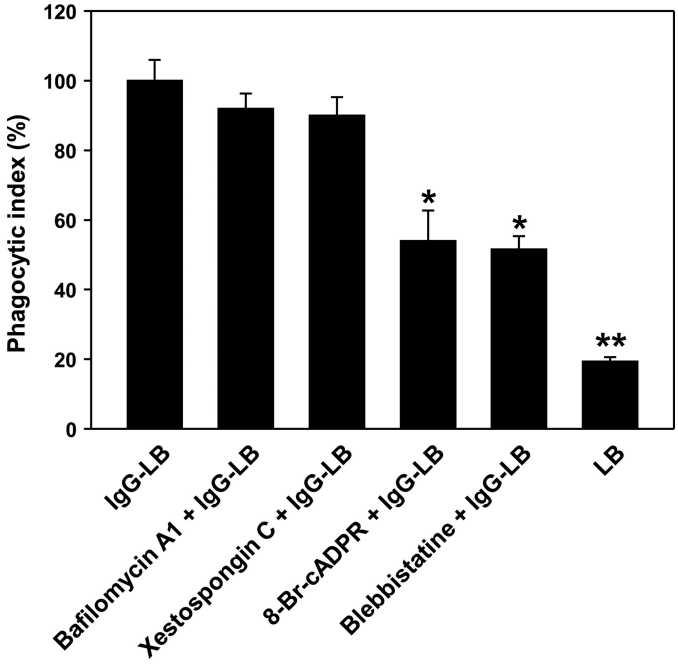

FIGURE 4. **Ca^{2+} signaling inhibitors greatly reduce FcγR-mediated phagocytosis in J774A.1 murine macrophages.** Phagocytic index was assessed by plating J774A.1 murine macrophages in 6-well plates and preincubating with the following inhibitors for 30 min as described under "Experimental Procedures": 600 nM bafilomycin A1, 2 μM xestospongin C, 100 μM 8-Br-cADPR, or 50 μM blebbistatin (magnification ×40). The data represent the mean ± S.D. of phagocytic ingestion of five experiments. $p < 0.01$ (*) and $p < 0.001$ (**) *versus* IgG-opsonized latex beads (*IgG-LB*).

stores (61). Surprisingly, this was not able to abrogate the long-lasting phase of the Ca^{2+} signal (Fig. 3*E*). CD38 is known to be activated via its internalization from the plasma membrane through its association with phosphorylated MHCIIA by protein kinase G (23). To verify this notion, we treated J774A.1 macrophages with a specific MHCIIA inhibitor, blebbistatin (62), which completely blocked the IgG-opsonized latex bead-induced Ca^{2+} signaling (Fig. 3*F*). These findings reveal that FcγR-mediated phagocytosis by way of IgG-opsonized latex beads induce Ca^{2+} signaling that is mediated by CD38/cADPR.

Ca^{2+} Signaling Inhibitors Greatly Reduce FcγR-mediated Phagocytosis in J774A.1 Murine Macrophages—Based on the Ca^{2+} signaling data, we proceeded to further quantify our results by calculating the phagocytic index of J774A.1 macrophages incubated under varying conditions for 30 min at 37 °C before inducing phagocytosis with IgG-opsonized latex beads (Fig. 4). Through microscopic imaging, we found that preincubation with bafilomycin A1 and xestospongin C did not significantly affect phagocytic capability, where full ingestion of IgG-opsonized latex beads was seen as in the untreated J774A.1 cells. This is concordant with our previous Ca^{2+} measurement data where these two inhibitors had no affect on the signaling. On the other hand, we observed a notable 46% decrease of phagocytosis when cells were preincubated with 8-Br-cADPR, where IgG-opsonized latex beads were seen mostly attached to the outer periphery of macrophages, and full internalization of the beads was decreased. Similar results were also obtained when macrophages were preincubated with the MHCIIA inhibitor, blebbistatin, where we found a 49% decrease. These observations affirm that cADPR is involved in FcγR-mediated phagocytosis in J774A.1 macrophages, and NAADP seems to not be a part of this particular signaling system.

J774A.1 Macrophages Utilize Store-operated Ca^{2+} Entry—It has been reported that store-operated Ca^{2+} entry (SOCE) may be involved in macrophage phagocytosis (63–67). To see which intracellular Ca^{2+} stores were present within J774A.1 cells, Ca^{2+} measurement was done on thapsigargin-induced Ca^{2+} release in a Ca^{2+} free buffer, where thapsigargin is a sarco/endoplasmic reticulum Ca^{2+}-ATPase (SERCA) inhibitor (67). This was able to cause a rapid release of Ca^{2+} from ER/SR stores, indicating their presence in the intracellular space (Fig. 5*A*). The addition of extracellular Ca^{2+} was also able to elicit a rapid influx of Ca^{2+}, suggesting the presence of Ca^{2+} channels. To see the contribution of acidic-like organelles, we performed Ca^{2+} measurements on GPN-induced Ca^{2+} release in a Ca^{2+}-free buffer as well (Fig. 5*B*). Unlike the thapsigargin-induced Ca^{2+} release, we were not able to detect any noticeable releases of intracellular Ca^{2+}, and the addition of extracellular Ca^{2+} did not cause any influx. This indicates a lack of role of acidic-like organelles as an intracellular Ca^{2+} store, which remains consistent with our earlier Ca^{2+} measurement, where bafilomycin A1 had no affect on FcγR-mediated phagocytosis.

To see which Ca^{2+} channels were involved, we performed Ca^{2+} measurement experiments using different Ca^{2+} channel inhibitors. We first preincubated J774A.1 macrophages with 10 μM nifedipine, which is a voltage-dependent L-type Ca^{2+} channel blocker (68). Surprisingly, this was not able to abrogate any increases of $[Ca^{2+}]_i$ in the cells (Fig. 5*C*). As a result, we used 50 μM concentration of another Ca^{2+} channel blocker, SK&F 96365, which also inhibits SOCE (69). Interestingly, this was able to abolish the Ca^{2+} signal; however, we were able to detect an initial sharp rise in Ca^{2+} (Fig. 5*D*). This similar pattern was also observed when the cells were treated in a Ca^{2+}-free buffer with 0.5 mM EGTA and was completely inhibited when treated in a Ca^{2+}-free buffer with 100 μM Fura-2AM (Fig. 5*E*), suggesting that the main method of Ca^{2+} influx from the extracellular environment may be mediated through the emptying of intracellular Ca^{2+} stores, hinting at a store-operated mechanism. To determine whether the initial Ca^{2+} peak is mediated by cADPR, J774A.1 cells were incubated with both SK&F 96365 and 8-Br-cADPR (Fig. 5*F*). Our results showed that this was able to effectively block any $[Ca^{2+}]_i$ rise in the cells. This outcome made us conclude that SOCE is involved during FcγR-mediated phagocytosis, where the initiator of extracellular Ca^{2+} influx is cADPR-mediated Ca^{2+} release from ER/SR stores.

To further explore the possible involvement of SOCE, various SOCE inhibitors were also preincubated with J774A.1 cells, and the phagocytic index was again measured (Fig. 5*H*). The SOCE channel blocker SK&F 96365 and thapsigargin were able to greatly reduce the number of internalized beads by 38 and 47%, respectively. The same was also seen when the phagocytic index was determined in a Ca^{2+}-free buffer with a 34% decrease in bead ingestion. These results further affirm our conclusion that FcγR-mediated phagocytosis in J774A.1 macrophages is controlled by both the mobilization of Ca^{2+} from intracellular Ca^{2+} stores as well as the influx of Ca^{2+} from the extracellular space through a Ca^{2+} channel.

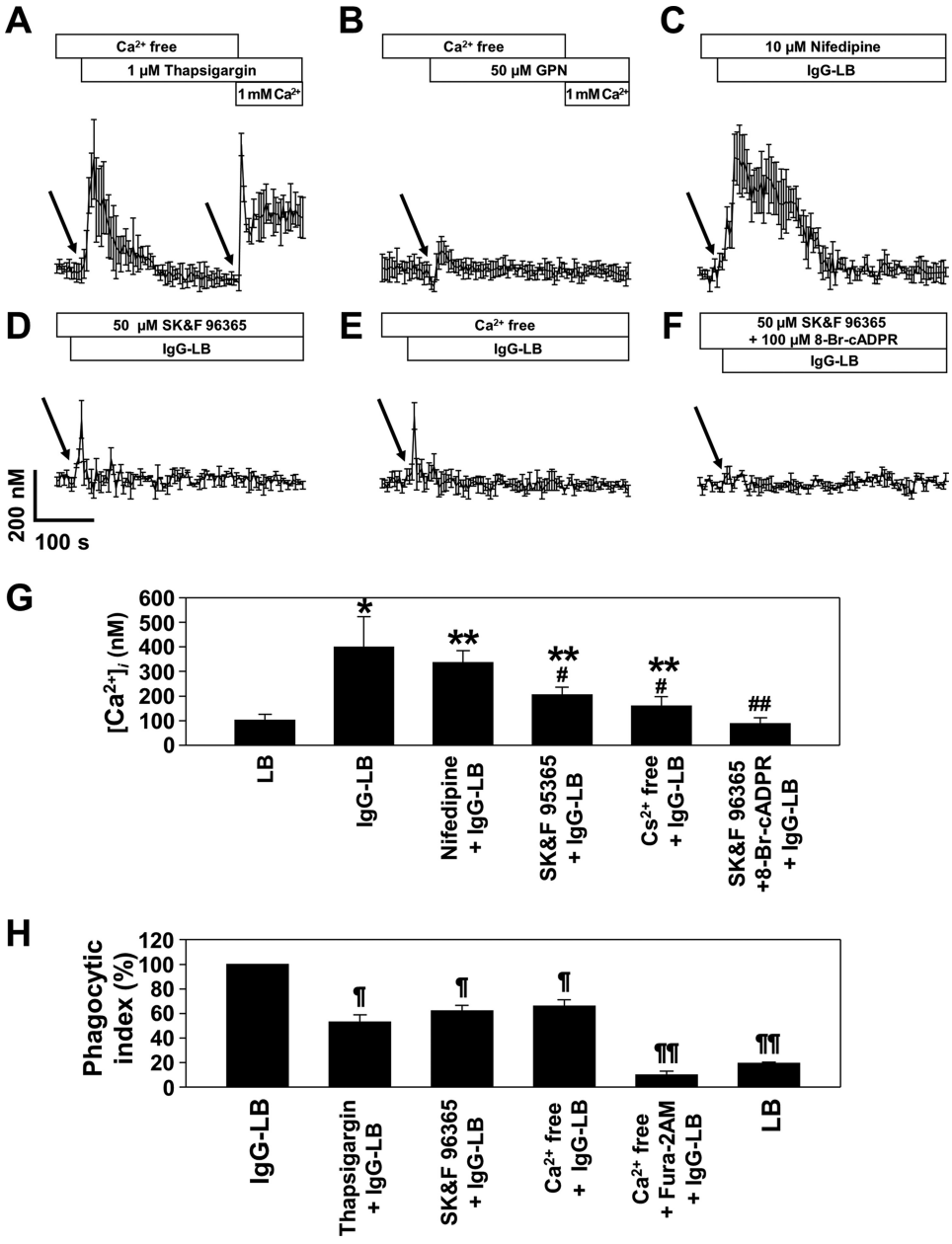

FIGURE 5. **J774A.1 murine macrophages utilize store-operated Ca^{2+} entry.** $[Ca^{2+}]_i$ measurements in FcγR stimulation to determine possible SOC mechanisms was determined by a confocal microscope on J774A.1 cells preincubated with Fluo-3 AM as described under "Experimental Procedures." J774A.1 murine macrophages were stimulated with 1 μM thapsigargin (*A*) or 50 μM GPN in the absence of extracellular calcium (*B*), and 5 min later 1 mM $CaCl_2$ was added to the medium. The *left arrow* indicates the time point of thapsigargin/bafilomycin addition. The *right arrow* indicates time point of 1 mM Ca^{2+} addition. $[Ca^{2+}]_i$ measurements in FcγR stimulation were further analyzed by preincubating cells with 10 μM nifedipine (*C*), 50 μM SK&F 96365 (*D*), Ca^{2+}-free buffer supplemented with 0.5 mM EGTA (*E*), and 50 μM SK&F 96365 with 100 μM 8-Br-cADPR (*F*). *Arrows* indicate the time point of opsonized latex bead addition. Each line represents the mean ± S.D. of $[Ca^{2+}]_i$ from minimum three independent experiments. *G*, shown is a direct comparison of Ca^{2+} levels at 15 s after treatment of LB or IgG-LB. Each line represents the mean ± S.D. of $[Ca^{2+}]_i$ from minimum three independent experiments. $p < 0.01$ (*) and $p < 0.05$ (**) *versus* LB treated group; $p < 0.05$ (#) and $p < 0.01$ (##) *versus* IgG-LB group. *H*, the phagocytic index was assessed by platting J774A.1 murine macrophages in 6-well plates and preincubating with the following inhibitors for 30 min as described under "Experimental Procedures": 1 μM thapsigargin, 50 μM SK&F 96365, Ca^{2+}-free buffer supplemented with 0.5 mM EGTA, or Ca^{2+}-free buffer supplemented with 100 μM Fura-2AM (magnification ×40). The data represent the mean ± S.D. of phagocytic ingestion of five experiments. $p < 0.01$ (¶) and $p < 0.001$ (¶¶) *versus* IgG-opsonized latex beads (*IgG-LB*).

FcγR-mediated Phagocytosis Induces cADPR Formation in J774A.1 Macrophages—Because our Ca^{2+} signaling data exhibited that 8-Br-cADPR was able to ablate the somewhat long-lasting Ca^{2+} signal and substantially reduce the phagocytic index, these considerations propelled us to measure $[cADPR]_i$ in J774A.1 macrophages after initiating FcγR-mediated phagocytosis with IgG-opsonized latex beads. We measured $[cADPR]_i$ within a time course and saw a significant rise in $[cADPR]_i$ within the first 5 s after IgG-opsonized latex bead addition, where levels remained elevated until 20 s, after which $[cADPR]_i$ tapered off to resting values (Fig. 6*A*). Interestingly, we were able to see a rise in $[cADPR]_i$ with unopsonized latex beads as well, although this increase was very slight, suggesting the possible involvement of cADPR in non-FcγR-mediated phagocytosis.

The use of bafilomycin A1 had no notable effects on both Ca^{2+} signaling and the phagocytic index of J774A.1 macro-

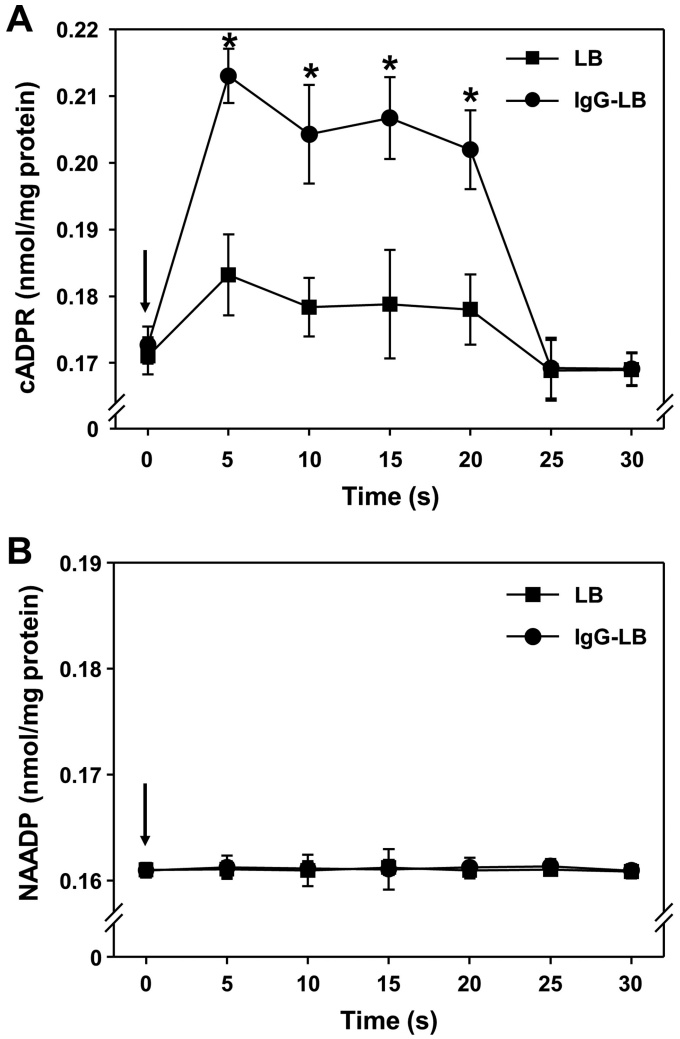

FIGURE 6. **FcγR-mediated phagocytosis induces cADPR formation in J774A.1 murine macrophages.** $[cADPR]_i$ and $[NAADP]_i$ was measured immediately after the addition of latex beads with or without IgG opsonization using a cycling assay as described under "Experimental Procedures." *A*, $[cADPR]_i$ increased in a time-dependent manner after initiating FcγR-mediated phagocytosis with IgG-opsonized latex beads. $p < 0.01$ (*) *versus* unopsonized latex beads (control LB). *B*, $[NAADP]_i$ increase was not detected after initiating FcγR-mediated phagocytosis with IgG-opsonized latex beads. Each line represents the mean ± S.D. of cADPR or NAADP formation from three independent experiments each.

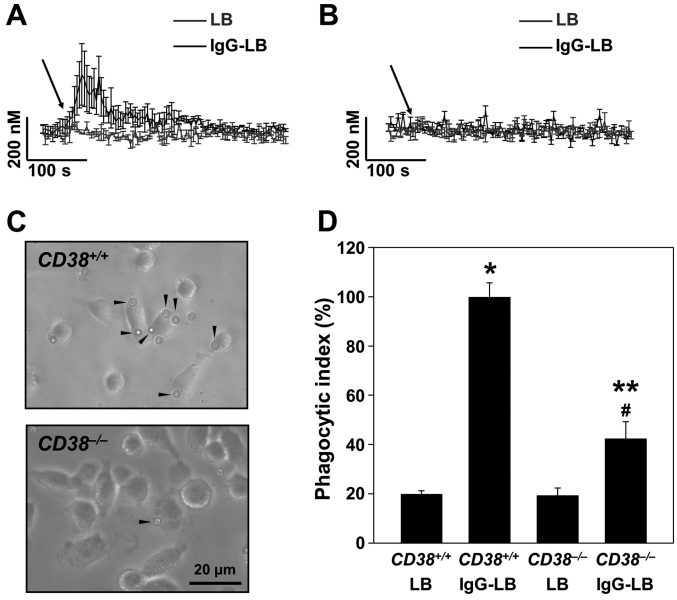

FIGURE 7. **$CD38^{-/-}$ mice macrophages have greatly reduced FcγR-mediated Ca^{2+} signals and phagocytosis.** $[Ca^{2+}]_i$ measurements in FcγR stimulation was determined by a confocal microscope on macrophages prepared from $CD38^{+/+}$ mice (*A*) and $CD38^{-/-}$ mice with LB or IgG-LB (*B*). *Arrows* indicate the time point of un/opsonized latex bead addition. Each line represents the mean ± S.D. of $[Ca^{2+}]_i$ from a minimum of three independent experiments. Phagocytosis was visualized by light microscopy in macrophages prepared from $CD38^{+/+}$ mice (*upper panel*) and $CD38^{-/-}$ mice (*lower panel*) (magnification ×40) (*C*). *D*, shown is quantification of the phagocytic index using opsonized (*IgG-LB*) or unopsonized (*LB*) latex beads in macrophages extracted from $CD38^{+/+}$ or $CD38^{-/-}$ mice. The data represent the mean ± S.D. of phagocytic ingestion of five experiments ($n = 15$). $p < 0.001$ (*) *versus* wild-type unopsonized latex bead ($CD38^{+/+}$-*LB*), $p < 0.05$ (**) *versus* CD38−/− unopsonized latex beads ($CD38^{-/-}$-*IgG LB*), and $p < 0.01$ (#) *versus* $CD38^{+/+}$ IgG opsonized latex beads ($CD38^{+/+}$-*IgG-LB*).

phages. To validate these observations, we also measured $[NAADP]_i$. Unsurprisingly, we were not able to detect any noticeable levels of $[NAADP]_i$ after evoking phagocytosis (Fig. 6*B*). This result remains in accordance with another finding that $[NAADP]_i$ is not detected in J774A.1 macrophages using another NAADP measurement method (70, 71). These aforementioned data made us conclude that FcγR-mediated phagocytosis with IgG-opsonized latex beads induces cADPR, but not NAADP, production.

IgG-opsonized Latex Beads Induces Ca^{2+} Signaling in Wild-type but Not in $CD38^{-/-}$ Mice—Because we have now established the role of Ca^{2+} signaling and a possible ADPR cyclase, such as CD38, in murine macrophage phagocytosis in an established cell line, we then tested these same principles *ex vivo* between wild-type and $CD38^{-/-}$ mice. Ca^{2+} signaling data using IgG-opsonized latex beads on extracted wild-type macrophages showed a typical Ca^{2+} response involving an initial and a somewhat long-lasting signal (Fig. 7*A*), very similar to what was previously noted in normal J774A.1 cells. The same Ca^{2+} signaling measurements were then performed on extracted $CD38^{-/-}$ macrophages, where we observed total ablation of any Ca^{2+} signal (Fig. 7*B*). These results suggest that CD38 is a possible candidate as an ADPR cyclase that is responsible for producing the Ca^{2+} signaling messengers necessary for allowing a rising level of $[Ca^{2+}]_i$.

$CD38^{-/-}$ Mouse Macrophage Has Greatly Reduced FcγR-mediated Phagocytosis—The results of our Ca^{2+} signaling data in both wild-type and $CD38^{-/-}$ macrophages prompted us to visually examine the differences in FcγR-mediated phagocytosis. Microscopic images of wild-type macrophages clearly show full engulfment of IgG-opsonized latex beads (Fig. 7*C*). Macrophages obtained from $CD38^{-/-}$ mice, however, showed a markedly impaired ability of the cells to commence phagocytosis, where little ingestion of opsonized particles was seen (Fig. 7*C*). Quantification of the data reveals that $CD38^{-/-}$ macrophages have a considerable decrement in the phagocytic index of more than 50% when compared with wild-type macrophages (Fig. 7*D*). This outcome again intimates that CD38 is the ADPR cyclase accountable for phagocytosis mediated by FcγR.

CD38 Deficiency Leads to Decreased Phagocytosis in Vivo—We further examined whether CD38 deficiency leads to compromising phagocytosis for live bacteria. We injected mice subcutaneously with *M. bovis* BCG and 3 weeks later injected

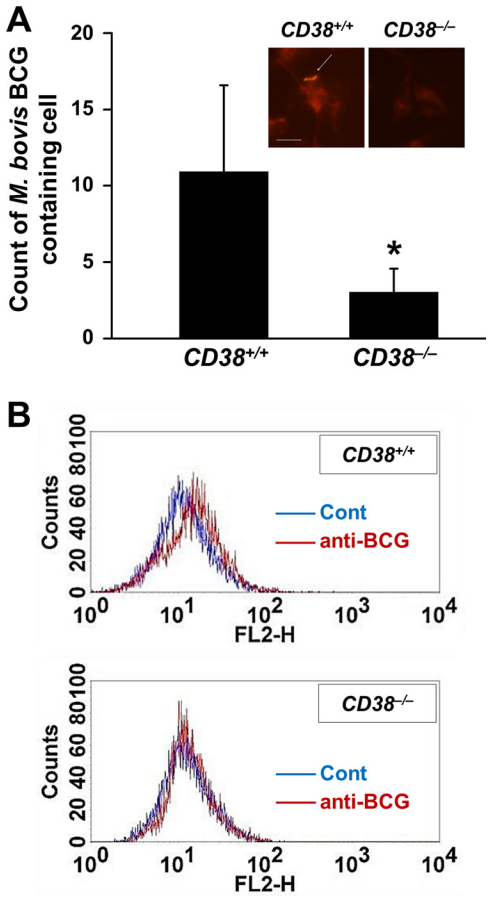

FIGURE 8. **CD38 deficiency leads to decreased phagocytosis *in vivo*.** *CD38*$^{+/+}$ and *CD38*$^{-/-}$ mice (each, $n = 5$) were injected subcutaneously with *M. bovis* BCG (1×10^7 colony-forming units/mouse). Three weeks later mice were injected intraperitoneal with opsonized *M. bovis* BCG (1×10^7 colony-forming units/mouse). Peritoneal macrophages were then isolated at 24 h after bacterial injection and stained with fluorescent auramine-rhodamine. *A*, cells containing phagocytic *M. bovis* BCG in five different fields for each condition were counted. Representative immunofluorescence images of three independent replicates are shown (*inset*). *Scale bars* = 10 μm. The *arrow* indicates auramine-rhodamine-stained *M. bovis* BCG. *B*, shown is flow cytometric analysis of phagocytic *M. bovis* BCG with biotinylated rabbit anti-BCG polyclonal antibody. Biotinylated antibody was detected with streptavidine-cy3 and analyzed with a flow cytometer. Streptavidine-Cy3 only was stained (*blue line*); biotinylated anti-BCG antibody and streptavidine-Cy3 were stained (*red line*). Data are expressed as mean ± S.D. $p < 0.001$ (*) *versus* *CD38*$^{+/+}$) ($n = 5$).

intraperitoneally with opsonized *M. bovis* BCG and compared phagocytic *M. bovis* BCG in peritoneal macrophages isolated after bacterial injection. Wild-type macrophages showed phagocytosed *M. bovis* BCG, whereas macrophages obtained from CD38$^{-/-}$ mice showed a significantly reduced phagocytic ingestion of *M. bovis* BCG (Fig. 8*A*). Flow cytometric analysis of phagocytic *M. bovis* BCG with biotinylated rabbit anti-BCG polyclonal antibody also shows no detectable phagocytic signal in macrophages obtained from CD38$^{-/-}$ mice compared with that in macrophages obtained from wild-type mice (Fig. 8*B*).

DISCUSSION

In this study our data clearly show the crucial role that CD38 has to play in regulating Ca^{2+} signals that is necessary for FcγR-mediated phagocytosis of IgG-opsonized latex beads. This is made possible through its internalization where the production of cADPR, but not NAADP, is allowed to take place. Although the role of IP_3, cADPR, and CD38 has been implied for immune cells in other works, a detailed investigation of the direct relationship between CD38 and FcγR-mediated phagocytosis in murine macrophages has not yet been made clear. We are also the first to show *ex vivo* the importance of CD38 and its necessary involvement in phagocytosis, where macrophages prepared from CD38$^{-/-}$ mice showed a non-existent Ca^{2+} signal as well as a drastically reduced uptake of IgG-opsonized latex beads as well as live bacteria. This is consistent with the phenotypic traits of CD38$^{-/-}$ mice where they tend to be more susceptible to infection and thus have a weaker survival rate (72). This could be due to the reduced ability for immune cells such as macrophages to uptake foreign microbes.

This is the first time to our knowledge that anyone has shown the possibility of CD38 being internalized along with the phagosome as it is endocytosed. It must be noted, however, that this was not always seen in our case, where we also observed the internalization of CD38 independently of the ingested IgG-opsonized latex bead. This internalization may be important in the physiological aspect because this will allow the rise in $[Ca^{2+}]_i$ to be more localized as seen in other Ca^{2+} studies with phagocytosis where there are spatial and temporal aspects to the signaling (72, 73), thus allowing for better control during phagocytic ingestion. This may be important for downstream effectors as a result of the increase in $[Ca^{2+}]_i$, such as Ca^{2+}-dependent gelsolin, an actin-binding protein, that has been documented to play a part in actin remodeling through assembly/disassembly during phagocytosis (29, 74–77). Whether there is a direct relationship between the Ca^{2+} that is induced by the CD38 product cADPR and gelsolin activity is highly likely but remains to be confirmed.

CD38 being internalized along with the phagosome-containing IgG-opsonized particles may have implications in not only phagocytic ingestion but in phagosome maturation as well. In one study with monocytes, a thin rim of high $[Ca^{2+}]_i$ was noted surrounding the phagosome of the ingested opsonized particles (76). We also observed this more localized form of $[Ca^{2+}]_i$ increase, unlike the more global rises seen in other systems. This confined Ca^{2+} around the phagosome during the later stages of phagocytosis has been implicated in oxidative enzyme-containing vesicle fusion with the phagosome (14, 27, 31) as well as ROS production (77–79) where blocking Ca^{2+} at this point impairs both. During these processes it is possible that CD38 may be an important player in providing the Ca^{2+} necessary for these events to take place, where its internalization can continue to produce cADPR at the local level.

Rapid cADPR production was seen during FcγR-mediated phagocytosis within a few seconds after initiation. This coincides with our NGD^+ assay where surface ADPR cyclase activity decreased in a time-dependent manner as well as our $[Ca^{2+}]_i$ level measurements, where it increased. This may seem contradictory especially in the context where it has been reported that it can take anywhere from 30 s to a few minutes for the actual phagocytosis process to begin (80). However; it must be again noted that CD38 can be internalized independently from the opsonized particles, as we have observed. So while the IgG-opsonized latex bead is being phagocytosed after binding to FcγRs, this can send a signaling cascade to the other surround-

ing CD38 to internalize, presumably via endosomes (81). This is what may be responsible for the quick production of $cADPR_i$ so that early Ca^{2+} signals can be generated in preparation for phagocytosis to take place. At present, we were not able to detect any distinguishable levels of $NAADP_i$, suggesting that Ca^{2+} generation in FcγR-mediated phagocytosis in murine macrophages relies solely on the action of cADPR on ER/SR Ca^{2+} stores.

SOCE seems to work synergistically with the release of intracellular Ca^{2+} from ER/SR stores with cADPR being the initiator of this Ca^{2+} mobilization. This is attributed to the fact that SOCE inhibitor SK&F 96365 in combination with 8-Br-cADPR effectively diminishes $[Ca^{2+}]_i$ levels and reduces the rate of IgG-opsonized latex bead phagocytic uptake. The usage of the L-type Ca^{2+} channel blocker nifedipine did not affect $[Ca^{2+}]_i$ levels in our study, suggesting that the Ca^{2+} channels contain characteristics that are more receptor-mediated or SOCE rather than voltage-gated. This is in accordance with another study where the usage of SK&F 96365 was able to eliminate the later rise in $[Ca^{2+}]_i$ levels and where another L-type Ca^{2+} channel blocker verapamil had no effect on *Listeria monocytogenes*-induced phagocytosis in J774A.1 murine macrophages (81, 82). The exact mechanism of intracellular Ca^{2+} store depletion-induced Ca^{2+} influx and the nature of the Ca^{2+} channel present on the cellular membrane remain yet to be discovered. Other Ca^{2+} channels such as Orai1 (83) and the ER Ca^{2+}-sensing protein STIM1 (61) have been implied to be involved in various immune cells. Whether or not CD38 works in tandem with these proteins and channels should warrant further investigation.

The main focus of this study was to investigate the role of CD38 in FcγR-mediated phagocytosis in the murine macrophage-like cell line J774A.1. We demonstrated that FcγR activation during IgG-opsonized latex bead ingestion elicits Ca^{2+} signaling through the production of cADPR by the internalization of the transmembrane ADP ribosyl cyclase CD38. Although the involvement of Ca^{2+} in phagocytosis is still up for debate, it should be indicated that there are countless of factors that affect macrophage phagocytosis as well as other Ca^{2+} signaling pathways that are involved in the process that are not strictly FcγR-mediated (84–88). Therefore, amid all the various works presently on Ca^{2+}-mediated phagocytosis, this study provides new perspectives in immune defense by introducing the involvement of the ADPR cyclase CD38 and can help shed light on developing novel methods or drugs that can help contain bacterial infections.

Acknowledgment—We thank Dong-Min Shin for technical support.

REFERENCES

1. Howard, M., Grimaldi, J. C., Bazan, J. F., Lund, F. E., Santos-Argumedo, L., Parkhouse, R. M., Walseth, T. F., and Lee, H. C. (1993) Formation and hydrolysis of cyclic ADP-ribose catalyzed by lymphocyte antigen CD38. *Science* **262,** 1056–1059
2. Lund, F., Solvason, N., Grimaldi, J. C., Parkhouse, R. M., and Howard, M. (1995) Murine CD38. An immunoregulatory ectoenzyme. *Immunol. Today* **16,** 469–473
3. Lee, H. C., Walseth, T. F., Bratt, G. T., Hayes, R. N., and Clapper, D. L. (1989) Structural determination of a cyclic metabolite of NAD^+ with intracellular Ca^{2+}-mobilizing activity. *J. Biol. Chem.* **264,** 1608–1615
4. Lee, H. C., and Aarhus, R. (1991) ADP-ribosyl cyclase. An enzyme that cyclizes NAD^+ into a calcium-mobilizing metabolite. *Cell Regul.* **2,** 203–209
5. Galione, A., Lee, H. C., and Busa, W. B. (1991) Ca^{2+}-induced Ca^{2+} release in sea urchin egg homogenates. Modulation by cyclic ADP-ribose. *Science* **253,** 1143–1146
6. Liu, D. Q., Guo, Y. L., Bian, Z., Chen, Y. Y., Chen, X., Liu, Y., Zhang, C. Y., and Zen, K. (2010) Uncoupling protein-2 negatively regulates polymorphonuclear leukocytes chemotaxis via modulating Ca^{2+} influx. *Arterioscler. Thromb. Vasc. Biol.* **30,** 575–581
7. Zabrenetzky, V., and Gallin, E. K. (1988) Inositol 1,4,5-trisphosphate concentrations increase after adherence in the macrophage-like cell line J774.1. *Biochem. J.* **255,** 1037–1043
8. Milara, J., Mata, M., Mauricio, M. D., Donet, E., Morcillo, E. J., and Cortijo, J. (2009) Sphingosine 1-phosphate increases human alveolar epithelial IL-8 secretion, proliferation, and neutrophil chemotaxis. *Eur. J. Pharmacol.* **609,** 132–139
9. Rah, S. Y., Mushtaq, M., Nam, T. S., Kim, S. H., and Kim, U. H. (2010) Generation of cyclic ADP-ribose and nicotinic acid adenine dinucleotide phosphate by CD38 for Ca^{2+} signaling in interleukin-8-treated lymphokine-activated killer cells. *J. Biol. Chem.* **285,** 21877–21887
10. Guse A. H., and Lee H. C. (2008) NAADP. A universal Ca^{2+} trigger. *Sci. Signal.* **1,** re10
11. Genazzani, A. A., and Galione, A. (1996) Nicotinic acid-adenine dinucleotide phosphate mobilizes Ca^{2+} from a thapsigargin-insensitive pool. *Biochem. J.* **315,** 721–725
12. Calcraft, P. J., Ruas, M., Pan, Z., Cheng, X., Arredouani, A., Hao, X., Tang, J., Rietdorf, K., Teboul, L., Chuang, K. T., Lin, P., Xiao, R., Wang, C., Zhu, Y., Lin, Y., Wyatt, C. N., Parrington, J., Ma, J., Evans, A. M., Galione, A., and Zhu, M. X. (2009) NAADP mobilizes calcium from acidic organelles through two-pore channels. *Nature* **459,** 596–600
13. Zhu, M. X., Ma, J., Parrington, J., Galione, A., and Evans, A. M. (2010) TPCs. Endolysosomal channels for Ca^{2+} mobilization from acidic organelles triggered by NAADP. *FEBS Lett.* **584,** 1966–1974
14. Churchill, G. C., Okada, Y., Thomas, J. M., Genazzani, A. A., Patel, S., and Galione, A. (2002) NAADP mobilizes Ca^{2+} from reserve granules, lysosome-related organelles, in sea urchin eggs. *Cell* **111,** 703–708
15. Galione A. (2006) NAADP, a new intracellular messenger that mobilizes Ca^{2+} from acidic stores. *Biochem. Soc. Trans.* **34,** 922–926
16. Park, K. H., Kim, B. J., Kang, J., Nam, T. S., Lim, J. M., Kim, H. T., Park, J. K., Kim, Y. G., Chae, S. W., and Kim, U. H. (2011) Ca^{2+} signaling tools acquired from prostasomes are required for progesterone-induced sperm motility. *Sci. Signal.* **4,** ra31
17. De Flora, A., Franco, L., Guida, L., Bruzzone, S., Usai, C., and Zocchi, E. (2000) Topology of CD38. *Chem. Immunol.* **75,** 79–98
18. Song, E. K., Rah, S. Y., Lee, Y. R., Yoo, C. H., Kim, Y. R., Yeom, J. H., Park, K. H., Kim, J. S., Kim, U. H., and Han, M. K. (2011) Connexin-43 hemichannels mediate cyclic ADP-ribose generation and its Ca^{2+}-mobilizing activity by NAD^+/cyclic ADP-ribose transport. *J. Biol. Chem.* **286,** 44480–44490
19. Orciani, M., Cavaletti, G., Fino, V., Mattioli-Belmonte, M., Tredici, G., Bruni, P., and Di Primio, R. (2008) Exploiting CD38-mediated endocytosis for immunoliposome internalization. *Anticancer Drugs.* **19,** 599–605
20. Trubiani, O., Guarnieri, S., Orciani, M., Salvolini, E., and Di Primio, R. (2004) Sphingolipid microdomains mediate CD38 internalization. Topography of the endocytosis. *Int. J. Immunopathol. Pharmacol.* **17,** 293–300
21. Funaro, A., Reinis, M., Trubiani, O., Santi, S., Di Primio, R., and Malavasi, F. (1998) CD38 functions are regulated through an internalization step. *J. Immunol.* **160,** 2238–2247
22. Zocchi, E., Usai, C., Guida, L., Franco, L., Bruzzone, S., Passalacqua, M., and De Flora, A. (1999) Ligand-induced internalization of CD38 results in intracellular Ca^{2+} mobilization. Role of NAD^+ transport across cell membranes. *FASEB J.* **13,** 273–283
23. Zocchi, E., Franco, L., Guida, L., Piccini, D., Tacchetti, C., and De Flora, A. (1996) NAD^+-dependent internalization of the transmembrane glycoprotein CD38 in human Namalwa B cells. *FEBS Lett.* **396,** 327–332

24. Rah, S. Y., Park, K. H., Nam, T. S., Kim, S. J., Kim, H., Im, M. J., and Kim, U. H. (2007) Association of CD38 with nonmuscle myosin heavy chain IIA and Lck is essential for the internalization and activation of CD38. *J. Biol. Chem.* **282,** 5653–5660
25. Niedergang, F., and Chavrier, P. (2004) Signaling and membrane dynamics during phagocytosis. Many roads lead to the phagos(R)ome. *Curr. Op. Cell Biol.* **16,** 422–428
26. Song, E. K., Lee, Y. R., Yu, H. N., Kim, U. H., Rah, S. Y., Park, K. H., Shim, I. K., Lee, S. J., Park, Y. M., Chung, W. G., Kim, J. S., and Han, M. K. (2008) Extracellular NAD is a regulator for FcγR-mediated phagocytosis in murine macrophages. *Biochem. Biophys. Res. Commun.* **367,** 156–161
27. Goldstein, I. M., Horn, J. K., Kaplan, H. B., and Weissmann, G. (1974) Calcium-induced lysozyme secretion from human polymorphonuclear leukocytes. *Biochem. Biophys. Res. Commun.* **60,** 807–812
28. Lew, P. D., Monod, A., Waldvogel, F. A., Dewald, B., Baggiolini, M., and Pozzan, T. (1986) Quantitative analysis of the cytosolic free calcium dependency of exocytosis from three subcellular compartments in intact human neutrophils. *J. Cell Biol.* **102,** 2197–2204
29. Valerius, N. H., Stendahl, O., Hartwig, J. H., and Stossel, T. P. (1981) Distribution of actin-binding protein and myosin in polymorphonuclear leukocytes during locomotion and phagocytosis. *Cell* **24,** 195–202
30. Yin, H. L., Albrecht, J. H., and Fattoum, A. (1981) Identification of gelsolin, a Ca^{2+}-dependent regulatory protein of actin gel-sol transformation, and its intracellular distribution in a variety of cells and tissues. *J. Cell Biol.* **91,** 901–906
31. Bengtsson, T., Jaconi, M. E., Gustafson, M., Magnusson, K. E., Theler, J. M., Lew, D. P., and Stendahl, O. (1993) Actin dynamics in human neutrophils during adhesion and phagocytosis is controlled by changes in intracellular free calcium. *Eur. J. Cell Biol.* **62,** 49–58
32. Jaconi, M. E., Lew, D. P., Carpentier, J. L., Magnusson, K. E., Sjögren, M., and Stendahl, O. (1990) Cytosolic free calcium elevation mediates the phagosome-lysosome fusion during phagocytosis in human neutrophils. *J. Cell Biol.* **110,** 1555–1564
33. Albert, R. K., Embree, L. J., McFeely, J. E., and Hickstein, D. D. (1992) Expression and function of β2 integrins on alveolar macrophages from human and nonhuman primates. *Am. J. Respir. Cell Mol. Biol.* **7,** 182–189
34. Hirsch, C. S., Ellner, J. J., Russell, D. G., and Rich, E. A. (1994) Complement receptor-mediated uptake and tumor necrosis factor-α-mediated growth inhibition of *Mycobacterium tuberculosis* by human alveolar macrophages. *J. Immunol.* **152,** 743–753
35. Taylor, M. E., and Drickamer, K. (1993) Structural requirements for high affinity binding of complex ligands by the macrophage mannose receptor. *J. Biol. Chem.* **268,** 399–404
36. Ezekowitz, R. A., Sastry, K., Bailly, P., and Warner, A. (1990) Molecular characterization of the human macrophage mannose receptor. Demonstration of multiple carbohydrate recognition-like domains and phagocytosis of yeasts in Cos-1 cells. *J. Exp. Med.* **172,** 1785–1794
37. Downing, J. F., Pasula, R., Wright, J. R., Twigg, H. L., 3rd, and Martin, W. J., 2nd (1995) Surfactant protein a promotes attachment of *Mycobacterium tuberculosis* to alveolar macrophages during infection with human immunodeficiency virus. *Proc. Natl. Acad. Sci.* **92,** 4848–4852
38. Dunne, D. W., Resnick, D., Greenberg, J., Krieger, M., and Joiner, K. A. (1994) The type I macrophage scavenger receptor binds to gram-positive bacteria and recognizes lipoteichoic acid. *Proc. Natl, Acad. Sci. U.S.A.* **91,** 1863–1867
39. Ravetch, J. V., and Bolland, S. (2001) IgG Fc receptors. *Annu. Rev. Immunol.* **19,** 275–290
40. Bermelin, M., and Decker, K. (1983) Ca^{2+} flux as an initial event in phagocytosis by rat Kupffer cells. *Eur. J. Biochem.* **131,** 539–543
41. Young, J. D., Ko, S. S., and Cohn, Z. A. (1984) The increase in intracellular free calcium associated with IgG γ2b/γ1 Fc receptor-ligand interactions. Role in phagocytosis. *Proc. Natl. Acad. Sci.* **81,** 5430–5434
42. Lew, D. P., Andersson, T., Hed, J., Di Virgilio, F., Pozzan, T., and Stendahl, O. (1985) Ca^{2+}-dependent and Ca^{2+}-independent phagocytosis in human neutrophils. *Nature* **315,** 509–511
43. Sawyer, D. W., Sullivan, J. A., and Mandell, G. L. (1985) Intracellular free calcium localization in neutrophils during phagocytosis. *Science* **230,** 663–666
44. Kusner, D. J., Hall, C. F., and Jackson, S. (1999) Fcγ receptor-mediated activation of phospholipase D regulates macrophage phagocytosis of IgG-opsonized particles. *J. Immunol.* **162,** 2266–2274
45. Nimmerjahn, F., Bruhns, P., Horiuchi, K., and Ravetch, J. V. (2005) FcγRIV. A novel FcR with distinct IgG subclass specificity. *Immunity* **23,** 41–51
46. Cooney, D. S., Phee, H., Jacob, A., and Coggeshall, K. M. (2001) Signal transduction by human-restricted Fc γ RIIa involves three distinct cytoplasmic kinase families leading to phagocytosis. *J. Immunol.* **167,** 844–854
47. Strzelecka-Kiliszek, A., Kwiatkowska, K., and Sobota, A. (2002) Lyn and Syk kinases are sequentially engaged in phagocytosis mediated by FcγR. *J. Immunol.* **169,** 6787–6794
48. Kiener, P. A., Rankin, B. M., Burkhardt, A. L., Schieven, G. L., Gilliland, L. K., Rowley, R. B., Bolen, J. B., and Ledbetter, J. A. (1993) Cross-linking of Fc γ receptor I (FcγRI) and receptor II (FcγRII) on monocytic cells activates a signal transduction pathway common to both Fc receptors that involves the stimulation of p72 Syk protein-tyrosine kinase. *J. Biol. Chem.* **268,** 24442–24448
49. Berridge, M. J. (1993) Inositol trisphosphate and calcium signaling. *Nature* **361,** 315–325
50. Graeff, R. M., Walseth, T. F., Fryxell, K., and Branton, W. D., Lee, H. C. (1994) Enzymatic synthesis and characterizations of cyclic GDP-ribose. A procedure for distinguishing enzymes with ADP-ribosyl cyclase activity. *J. Biol. Chem.* **269,** 30260–30267
51. Tsien, R. Y., Pozzan, T., and Rink, T. J. (1982) T-cell mitogens cause early changes in cytoplasmic-free Ca^{2+} and membrane potential in lymphocytes. *Nature* **295,** 68–71
52. Desjardins M., Celis J. E., van Meer G., Dieplinger H., Jahraus A., Griffiths G., and Huber L. A. (1994) Molecular characterization of phagosomes. *J. Biol. Chem.* **269,** 32194–32200
53. Shui W., Sheu L., Liu J., Smart B., Petzold C. J., Hsieh T. Y., Pitcher A., Keasling J. D., and Bertozzi C. R. (2008) Membrane proteomics of phagosomes suggests a connection to autophagy. *Proc. Natl. Acad. Sci. U.S.A.* **105,** 16952–16957
54. Graeff, R., and Lee, H. C. (2002) A novel cycling assay for cellular cADP-ribose with nanomolar sensitivity. *Biochem. J.* **361,** 379–384
55. Graeff, R. M., and Lee, H. C. (2003) High throughput fluorescence-based assays for cyclic ADP-ribose, NAADP, and their metabolic enzymes. *Comb. Chem. High Throughput Screen.* **6,** 367–379
56. Koval, M., Preiter, K., Adles, C., Stahl, P. D., and Steinberg, T. H. (1998) Size of IgG-opsonized particles determines macrophage response during internalization. *Exp. Cell Res.* **242,** 265–273
57. Miyamoto, S., Izumi, M., Hori, M., Kobayashi, M., and Ozaki, H., Karaki, H. (2000) Xestospongin C, a selective and membrane-permeable inhibitor of IP_3 receptor, attenuates the positive inotropic effect of α-adrenergic stimulation in guinea pig papillary muscle. *Br. J. Pharmacol.* **130,** 650–654
58. Rakovic, S., Cui, Y., Iino, S., Galione, A., Ashamu, G. A., Potter, B. V., and Terrar, D. A. (1999) An antagonist of cADP-ribose inhibits arrhythmogenic oscillations of intracellular Ca^{2+} in heart cells. *J. Biol. Chem.* **274,** 17820–17827
59. Lee, H. C., Aarhus, R., Graeff, R., Gurnack, M. E., and Walseth, T. F. (1994) Cyclic ADP ribose activation of the ryanodine receptor is mediated by calmodulin. *Nature* **370,** 307–309
60. Pan, Z., Damron, D., Nieminen, A. L., Bhat, M. B., and Ma, J. (2000) Depletion of intracellular Ca^{2+} by caffeine and ryanodine induces apoptosis of Chinese hamster ovary cells transfected with ryanodine receptor. *J. Biol. Chem.* **275,** 19978–19984
61. Bowman, E. J., Siebers, A., and Altendorf, K. (1988) Bafilomycins. A class of inhibitors of membrane ATPases from microorganisms, animal cells, and plant cells. *Proc. Natl. Acad. Sci.* **85,** 7972–7976
62. Kovács, M., Tóth, J., Hetényi, C., Málnási-Csizmadia A, and Sellers, J. R. (2004) Mechanism of blebbistatin inhibition of myosin II. *J. Biol. Chem.* **279,** 35557–35563
63. Braun, A., Gessner, J. E., Varga-Szabo, D., Syed, S. N., Konrad, S., Stegner, D., Vögtle, T., Schmidt, R. E., and Nieswandt, B. (2009) STIM1 is essential for Fcγ receptor activation and autoimmune inflammation. *Blood* **113,** 1097–1104

64. Lieberman, L. A., and Higgins, D. E. (2009) A small-molecule screen identifies the antipsychotic drug pimozide as an inhibitor of *Listeria monocytogenes* infection. *Antimicrob. Agents Chemother.* **53,** 756–764
65. Cuttell, L., Vaughan, A., Silva, E., Escaron, C. J., Lavine, M., Van Goethem, E., Eid, J. P., Quirin, M., and Franc, N. C. (2008) Undertaker, a *Drosophila* Junctophilin, links Draper-mediated phagocytosis and calcium homeostasis. *Cell* **135,** 524–534
66. Link, T. M., Park, U., Vonakis, B. M., Raben, D. M., Soloski, M. J., and Caterina, M. J. (2010) TRPV2 has a pivotal role in macrophage particle binding and phagocytosis. *Nat. Immunol.* **11,** 232–239
67. Lytton, J., Westlin, M., and Hanley, M. R. (1991) Thapsigargin inhibits the sarcoplasmic or endoplasmic reticulum Ca-ATPase family of calcium pumps. *J. Biol. Chem.* **266,** 17067–17071
68. Blitzer, R. D., Gil, O., Omri, G., and Landau, E. M. (1991) Nifedipine blocks calcium-dependent cholinergic depolarization in the guinea pig hippocampus. *Brain Res.* **542,** 293–299
69. Merritt, J. E., Armstrong, W. P., Benham, C. D., Hallam, T. J., Jacob, R., Jaxa-Chamiec, A., Leigh, B. K., McCarthy, S. A., Moores, K. E., and Rink, T. J. (1990) SK&F 96365, a novel inhibitor of receptor-mediated calcium entry. *Biochem. J.* **271,** 515–522
70. Churamani, D., Carrey, E. A., Dickinson, G. D., and Patel, S. (2004) Determination of cellular nicotinic acid-adenine dinucleotide phosphate (NAADP) levels. *Biochem. J.* **380,** 449–454
71. Marks, P. W., and Maxfield, F. R. (1990) Local and global changes in cytosolic-free calcium in neutrophils during chemotaxis and phagocytosis. *Cell Calcium.* **11,** 181–190
72. Partida-Sánchez, S., Cockayne, D. A., Monard, S., Jacobson, E. L., Oppenheimer, N., Garvy, B., Kusser, K., Goodrich, S., Howard, M., Harmsen, A., Randall, T. D., and Lund, F. E. (2001) Cyclic ADP-ribose production by CD38 regulates intracellular calcium release, extracellular calcium influx, and chemotaxis in neutrophils and is required for bacterial clearance *in vivo*. *Nat. Med.* **7,** 1209–1216
73. Stendahl, O., Krause, K. H., Krischer, J., Jerström, P., Theler, J. M., Clark, R. A., Carpentier, J. L., and Lew, D. P. (1994) Redistribution of intracellular Ca^{2+} stores during phagocytosis in human neutrophils. *Science* **265,** 1439–1441
74. Serrander, L., Skarman, P., Rasmussen, B., Witke, W., Lew, D. P., Krause, K. H., Stendahl, O., and Nüsse, O. (2000) Selective inhibition of IgG-mediated phagocytosis in gelsolin-deficient murine neutrophils. *J. Immunol.* **165,** 2451–3457
75. Arora, P. D., Chan, M. W., Anderson, R. A., Janmey, P. A., and McCulloch, C. A. (2005) Separate functions of gelsolin mediate sequential steps of collagen phagocytosis. *Mol. Biol. Cell.* **16,** 5175–5190
76. Kim, E., Enelow, R. I., Sullivan, G. W., and Mandell, G. L. (1992) Regional and generalized changes in cytosolic-free calcium in monocytes during phagocytosis. *Infect. Immun.* **60,** 1244–1248
77. Elferink, J. G. (1982) Interference of the calcium antagonists verapamil and nifedipine with lysosomal enzyme release from rabbit polymorphonuclear leukocytes. *Arzneimittelforschung* **32,** 1417–1420
78. Dieter, P., Fitzke, E., and Duyster, J. (1993) BAPTA induces a decrease of intracellular-free calcium and a translocation and inactivation of protein kinase C in macrophages. *Biol. Chem. Hoppe Seyler* **374,** 171–174
79. Wilsson, A., Lundqvist, H., Gustafsson, M., and Stendahl, O. (1996) Killing of phagocytosed *Staphylococcus aureus* by human neutrophils requires intracellular free calcium. *J. Leukoc. Biol.* **59,** 902–907
80. Matsumura, K., Orita, K., Wakamoto, Y., and Yasuda, K. (2006) Phagocytic response to fully controlled plural stimulation of antigens on macrophage using on-chip microcultivation system. *J. Nanobiotechnology* **4,** 7
81. Muñoz, P., Mittelbrunn, M., de la Fuente, H., Pérez-Martínez, M., García-Pérez, A., Ariza-Veguillas A, Malavasi, F., Zubiaur, M., Sánchez-Madrid, F., and Sancho, J. (2008) Antigen-induced clustering of surface CD38 and recruitment of intracellular CD38 to the immunologic synapse. *Blood.* **111,** 3653–3664
82. Wadsworth, S. J., and Goldfine, H. (1999) *Listeria monocytogenes* phospholipase C-dependent calcium signaling modulates bacterial entry into J774 macrophage-like cells. *Infect. Immun.* **67,** 1770–1778
83. Schaff, U. Y., Dixit, N., Procyk, E., Yamayoshi, I., Tse, T., and Simon, S. I. (2010) Orai1 regulates intracellular calcium, arrest, and shape polarization during neutrophil recruitment in shear flow. *Blood* **115,** 657–666
84. McLeish, K. R., Dean, W. L., Wellhausen, S. R., and Stelzer, G. T. (1989) Role of intracellular calcium in priming of human peripheral blood monocytes by bacterial lipopolysaccharide. *Inflammation* **13,** 681–692
85. Klein, J. B., Payne, V., Schepers, T. M., and McLeish, K. R. (1990) Bacterial lipopolysaccharide enhances polymorphonuclear leukocyte function independent of changes in intracellular calcium. *Inflammation* **14,** 599–611
86. Rosales, C., and Brown, E. J. (1991) Two mechanisms for IgG Fc receptor-mediated phagocytosis by human neutrophils. *J. Immunol.* **146,** 3937–3944
87. Ichinose, M., Asai, M., and Sawada, M. (1995) β-Endorphin enhances phagocytosis of latex particles in mouse peritoneal macrophages. *Scand. J. Immunol.* **42,** 311–316
88. Ichinose, M., Asai, M., and Sawada, M. (1995) Enhancement of phagocytosis by dynorphin A in mouse peritoneal macrophages. *J. Neuroimmunol.* **60,** 37–43